

Adaptive aneuploidy protects against thiol peroxidase deficiency by increasing respiration via key mitochondrial proteins

Alaattin Kaya^a, Maxim V. Gerashchenko^a, Inge Seim^a, Jean Labarre^b, Michel B. Toledano^b, and Vadim N. Gladyshev^{a,1}

^aDivision of Genetics, Department of Medicine, Brigham and Women's Hospital and Harvard Medical School, Boston, MA 02115; and ^bOxidative Stress and Cancer, Institut de Biologie et Technologie-Saclay, FRE3377 Commissariat à l'Energie Atomique (CEA), Centre National de la Recherche Scientifique (CNRS), Université Paris-Sud, CEA-Saclay, F-91191 Gif Sur Yvette, France

Edited by Angelika Amon, Massachusetts Institute of Technology, Cambridge, MA, and approved July 10, 2015 (received for review March 16, 2015)

Aerobic respiration is a fundamental energy-generating process; however, there is cost associated with living in an oxygen-rich environment, because partially reduced oxygen species can damage cellular components. Organisms evolved enzymes that alleviate this damage and protect the intracellular milieu, most notably thiol peroxidases, which are abundant and conserved enzymes that mediate hydrogen peroxide signaling and act as the first line of defense against oxidants in nearly all living organisms. Deletion of all eight thiol peroxidase genes in yeast ($\Delta 8$ strain) is not lethal, but results in slow growth and a high mutation rate. Here we characterized mechanisms that allow yeast cells to survive under conditions of thiol peroxidase deficiency. Two independent $\Delta 8$ strains increased mitochondrial content, altered mitochondrial distribution, and became dependent on respiration for growth but they were not hypersensitive to H_2O_2 . In addition, both strains independently acquired a second copy of chromosome XI and increased expression of genes encoded by it. Survival of $\Delta 8$ cells was dependent on mitochondrial cytochrome-c peroxidase (*CCP1*) and *UTH1*, present on chromosome XI. Coexpression of these genes in $\Delta 8$ cells led to the elimination of the extra copy of chromosome XI and improved cell growth, whereas deletion of either gene was lethal. Thus, thiol peroxidase deficiency requires dosage compensation of *CCP1* and *UTH1* via chromosome XI aneuploidy, wherein these proteins support hydroperoxide removal with the reducing equivalents generated by the electron transport chain. To our knowledge, this is the first evidence of adaptive aneuploidy counteracting oxidative stress.

thiol peroxidase | oxidative stress | aneuploidy | respiration

Several fundamental biological processes such as respiration, photosynthesis, and the immune response, as well as numerous other cellular processes, lead to the production of partially reduced species of molecular oxygen known as reactive oxygen species (ROS) (1, 2). Elevated levels of ROS are often associated with oxidative stress, which manifests as damage to lipids, proteins, DNA, metabolites, and other biomolecules (3). However, ROS are not only deleterious factors but may also participate in the regulation of cellular processes. For example, hydrogen peroxide (H_2O_2)-mediated oxidation of cysteine residues is involved in redox signaling (4, 5). Therefore, it is important for organisms to carefully control redox homeostasis.

To deal with the dual role of ROS as deleterious or beneficial species, organisms have evolved several mechanisms. Protectors from ROS, known as antioxidants, can be categorized as non-enzymatic and enzymatic ROS molecules. The nonenzymatic antioxidants buffer the intracellular milieu against ROS toxicity. For example, ascorbate, tocopherol, flavonoids, alkaloids, and carotenoids can scavenge oxygen-derived free radicals, whereas glutathione (GSH), a highly abundant tripeptide, supports two electron reduction mechanisms (6). Enzyme antioxidants include superoxide dismutases (eliminate the superoxide radical) and catalases (eliminate H_2O_2), as well as many other enzymes (6).

Notable among them are peroxiredoxins (Prxs) and glutathione peroxidases (Gpxs), two families of thiol-specific peroxide scavengers (7) collectively known as thiol peroxidases. Prxs and Gpxs are highly conserved, and many organisms have multiple copies of these genes. For example, five Prxs and three Gpxs, localized to different cellular compartments, have been identified in *Saccharomyces cerevisiae* (8). One of the most deleterious damage forms inflicted by ROS is DNA damage (9). Many genetic disorders as well as different forms of cancer are associated with oxidative stress-induced DNA damage (10, 11). Recent studies offer direct proof that thiol peroxidases represent the first line of defense against oxidative stress-induced DNA damage (12, 13).

The observation that compromised function of thiol peroxidases causes the loss of genome stability and a broad spectrum of mutations and chromosomal rearrangements has provided further evidence that these enzymes are significant contributors to genome stability (14, 15). Aneuploidy, with its aberrant number of chromosomes, is also associated with oxidative stress (16); however, a link between thiol peroxidase status and aneuploidy has not been reported previously.

Significance

Aneuploidy, a condition of abnormal chromosomal content, can support adaptive mechanisms in response to environmental cues but comes at the expense of decreased proliferation and dysfunction of cellular processes. Here we show that the gain of an extra copy of chromosome XI in yeast is an adaptive mechanism to deal with oxidative stress under conditions of antioxidant deficiency. We narrowed down the effect of adaptive aneuploidy to two genes on chromosome XI, which supported increased mitochondrial abundance and respiration, which in turn provided reducing equivalents for hydroperoxide removal. Forced expression of these genes eliminated aneuploidy, improved cell growth, and was sufficient for protection against oxidative stress. Thus, aneuploidy can adaptively reprogram cellular metabolism, protecting against oxidative stress by upregulating respiration.

Author contributions: A.K. and V.N.G. designed research; A.K., M.V.G., and J.L. performed research; A.K., M.V.G., I.S., M.B.T., and V.N.G. analyzed data; and A.K. and V.N.G. wrote the paper.

The authors declare no conflict of interest.

This article is a PNAS Direct Submission.

Data deposition: The genome reads reported in this paper have been deposited in the BioProject database, www.ncbi.nlm.nih.gov/bioproject (accession no. PRJNA287442). Transcriptome (RNA-sequencing) reads and fragments per kilobase of transcript per million mapped read values have been deposited in the Gene Expression Omnibus (GEO) database, www.ncbi.nlm.nih.gov/geo (accession no. GSE70036). Ribosome profiling (Ribosequencing) data have also been deposited in the GEO database (accession no. GSE59573).

¹To whom correspondence should be addressed. Email: vgladyshev@rics.bwh.harvard.edu.

This article contains supporting information online at www.pnas.org/lookup/suppl/doi:10.1073/pnas.1505315112/-DCSupplemental.

Recently, we isolated two independent strains lacking all eight thiol peroxidase genes ($\Delta 8$ cells) (15). In the current study, we investigated how these cells deal with hydroperoxides. We found that both $\Delta 8$ mutants were strictly dependent on respiration and were characterized by chromosome XI (chr-XI) aneuploidy. Two genes, *CCP1* and *UTH1*, located on this chromosome were responsible for the whole-chromosome duplication, because they allowed H_2O_2 elimination with the reducing equivalents of the electron transport chain (ETC). These two genes were essential for these cells, whereas their forced coexpression in $\Delta 8$ mutants allowed cells to lose the extra copy of chr-XI and increase their growth. These findings identify a mechanism of adaptive aneuploidy, which in turn points to new targets for therapeutic interventions for diseases associated with oxidative stress.

Results

Characterization of $\Delta 8$ Strains. Our previous analyses of $\Delta 8$ cells revealed that thiol peroxidases are not essential; however, they surprisingly could withstand several stresses (17). Two independent $\Delta 8$ isolates also manifested phenotypes such as slow growth, short lifespan, and decreased colony size. We confirmed that both isolates grew slower than wild-type (Wt) cells but were nearly as resistant to treatment with 0.4 mM H_2O_2 as Wt cells (Fig. 1A). An additional observation was that $\Delta 8$ cells were dependent on respiration, as these cells were highly sensitive to antimycin-A, rotenone, and oligomycin (Fig. 1B). Consistent with the dependence on respiration, both $\Delta 8$ isolates increased their mitochondrial copy number, as measured by the ratio of mitochondrial DNA (mtDNA) to nuclear DNA (Fig. 1C). Mitochondria are known to be the major source of ROS (18); therefore, it was surprising that thiol peroxidase deficiency led to a higher, rather than lower, mitochondrial content, and forced cells to rely on respiration when grown on rich medium. We also observed structural differences in mitochondria distribution between Wt and $\Delta 8$ cells: Logarithmically grown Wt cells showed filamentous structure of mitochondria, whereas $\Delta 8$ cells exhibited punctuated mitochondria and mitochondrial clusters (Fig. 1D). Together, these data and the

fact that the observed phenotypes appeared in two independent $\Delta 8$ isolates suggest that increased respiration is an adaptive feature of $\Delta 8$ cells.

Chr-XI Aneuploidy in $\Delta 8$ Cells. Genomic sequencing of Wt cells revealed uniform coverage of reads across the genome, as expected; however, both $\Delta 8$ strains had twice as many reads corresponding to chr-XI (Fig. 2A). As a control, we sequenced the genome and analyzed the growth and sensitivity to respiration inhibitors of the Wt-M11 strain, which is characterized by duplication of chr-XI and has a complete set of thiol peroxidase genes. This strain was not sensitive to inhibitors of respiration (Fig. 1B), but its genome coverage was identical to that of $\Delta 8$ strains (Fig. 2A). In contrast, genome sequencing of cells lacking all five Prxs ($\Delta 5$ cells) or all three Gpxs ($\Delta 3$ cells), which served as the initial strains for independent preparation of the two $\Delta 8$ isolates, did not show increased chr-XI coverage (Fig. 2A). Thus, the two $\Delta 8$ strains independently acquired a second copy of chr-XI and are characterized by aneuploidy.

Previous studies showed that genes encoded on duplicated chromosomes tend to be more highly expressed (19, 20). Indeed, the second copy of chr-XI was fully transcriptionally active in $\Delta 8$ cells, as revealed by RNA-seq (sequencing) analyses (Fig. 2B and Dataset S1). The expression of genes encoded by chr-XI were, on average, twice as high in these cells compared with Wt cells (Fig. 2C), whereas the average gene expression derived from other chromosomes was unchanged. This observation was also confirmed by examining gene expression in Wt-M11 cells (Fig. 2B). Thus, there was a direct correspondence between chromosome copy number and derived gene expression in $\Delta 8$ strains, as shown previously for cells with other mutant backgrounds (20, 21).

Elevated Expression of Chr-XI Genes *SRX1*, *CCP1*, and *UTH1* Is a Common Feature of $\Delta 8$ Strains. Given the fact that aneuploidy can cause rapid adaptive evolution (22, 23), we investigated the possibility that chr-XI disomy, observed in $\Delta 8$ strains, was the primary genetic adaptation that accounts for the observed phenotypes of $\Delta 8$ cells and, perhaps, for their viability, resistance to oxidative stress, and dependence on respiration. First, we compared global gene expression between the $\Delta 8$ strains. The pair of $\Delta 8$ strains with identical karyotypes displayed a highly similar transcriptome profile ($\rho = 0.97$), whereas both showed significant changes in gene expression compared with Wt cells (15). A better reference strain to identify genes whose expression changed in response to thiol peroxidase deficiency, as opposed to changes in response to aneuploidy, is the Wt-M11 strain. With this idea in mind, we identified three genes (*SRX1*, *CCP1*, and *UTH1*) whose expression deviated significantly in both $\Delta 8$ strains compared with either Wt-M11 cells ($P < 0.01$) or Wt cells (Fig. 2D–F). *Srx1* is responsible for reducing the hyperoxidized catalytic cysteine of Tsa1 and Tsa2 (24), two of the thiol peroxidases that were deleted in $\Delta 8$ strains. Thus, the increased expression of *SRX1* is likely a response to the loss of Prx functions. *CCP1* encodes a heme-containing protein, which occurs in the mitochondrial intermembrane space and functions in respiring mitochondria (25, 26). It was found that Ccp1 is an efficient H_2O_2 scavenger that uses cytochrome *c* as a reductant and protects respiring yeast cells from H_2O_2 (27). The SUN family protein Uth1 (*UTH1*) is a mitochondrial inner-membrane protein that is thought to be involved in mitochondrial biogenesis, aging, cell death, and oxidative stress response (28–30). It is of interest that all three identified genes are important for mitochondrial function and protection against oxidative stress.

***CCP1* and *UTH1* but Not *SRX1* Are Essential for $\Delta 8$ Viability.** Gene expression analyses suggested that the elevated expression of the three genes might be an adaptation of $\Delta 8$ cells to thiol peroxidase deficiency. If so, $\Delta 8$ cells may require these genes for viability. To

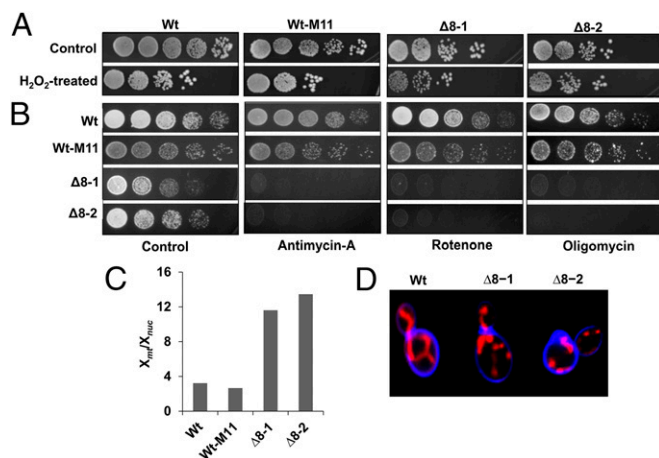


Fig. 1. Phenotypes of $\Delta 8$ strains. (A) H_2O_2 tolerance. Tenfold serial dilution of Wt cells, Wt-M11 cells, and two independent $\Delta 8$ mutant isolates ($\Delta 8$ -1 and $\Delta 8$ -2) onto YPD plates containing (H_2O_2 -treated) or not (control) 0.4 mM H_2O_2 . Pictures were taken after 3 d. (B) Dependence on respiration. Tenfold serial dilution assays of Wt, Wt-M11, $\Delta 8$ -1, and $\Delta 8$ -2 cells in the presence or absence of antimycin-A, rotenone, and oligomycin. (C) Increased mtDNA copy number in $\Delta 8$ mutant cells. The ratio of the normalized number of reads corresponding to mtDNA (X_{mt}) and the normalized number of reads corresponding to nuclear DNA (X_{nu}) is shown for each strain. (D) Distribution of mitochondria. Mitochondria were stained with MitoTracker Red. Blue color corresponds to calcofluor, which visualizes cell membranes.

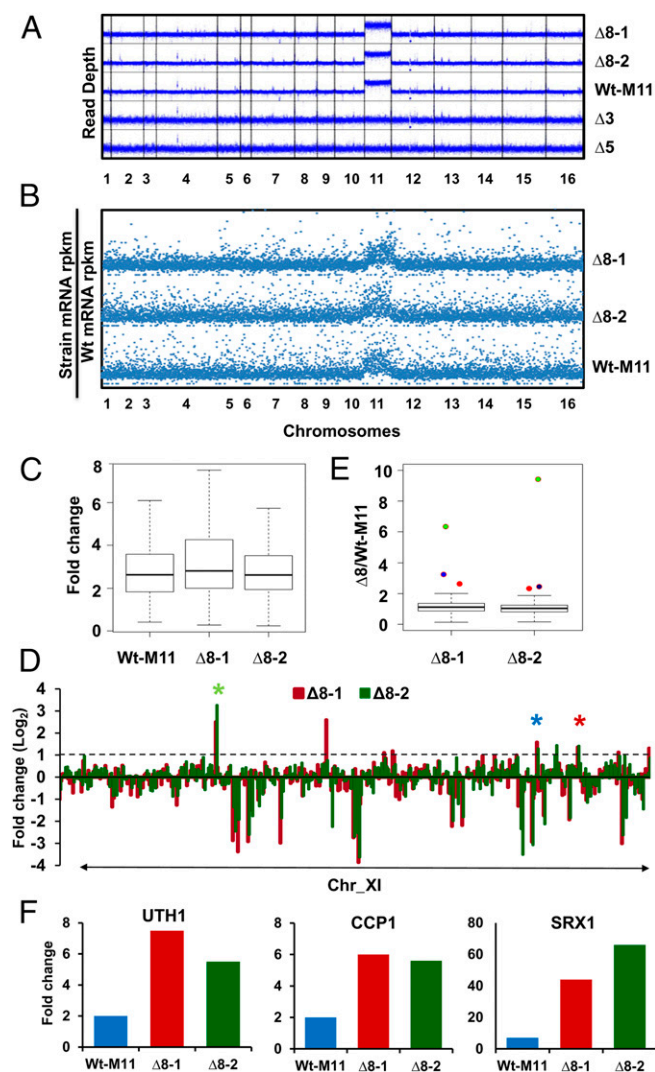


Fig. 2. Chromosome XI aneuploidy of $\Delta 8$ cells. (A) Occurrence of chr-XI disomy in $\Delta 8$ strains identified by genome sequencing. Read depth was calculated in 100-bp windows. Genome coverage is shown for two independent $\Delta 8$ mutant isolates ($\Delta 8$ -1 and $\Delta 8$ -2), a chr-XI aneuploid strain (Wt-M11), and strains ($\Delta 3$, lacking three Gpxs; $\Delta 5$, lacking five Prxs) from which $\Delta 8$ cells were prepared. (B) Increased expression of chr-XI genes revealed by RNA-seq. Total numbers of normalized FPKM reads per strain were normalized by Wt reads, and the ratio was plotted. (C) Increased average expression of chr-XI genes in Wt-M11, $\Delta 8$ -1, and $\Delta 8$ -2 cells. Average expression of genes on chr-XI of Wt-M11, $\Delta 8$ -1, and $\Delta 8$ -2 strains was calculated as fold change compared with Wt cells. Center black bar indicates median and error bars (whiskers) indicate 95% confidence interval for C and E. (D) Expression levels of genes on chr-XI in $\Delta 8$ cells compared with those in the Wt-M11 strain. Log₂ ratios of FPKM read values per gene are shown for chr-XI of $\Delta 8$ -1 (red) and $\Delta 8$ -2 (green) cells. Three target genes that increased expression in both $\Delta 8$ strains more than twofold are labeled with asterisks [*SRX1* (green), *UTH1* (blue), and *CCP1* (red)]. (E) Analysis of gene expression on chr-XI. The $\Delta 8$ /Wt-M11 gene expression ratios were analyzed for all chr-XI genes of $\Delta 8$ -1 and $\Delta 8$ -2 strains. Expression of the three genes that showed increased expression in both $\Delta 8$ strains, *SRX1* (green), *UTH1* (blue), and *CCP1* (red), is indicated with dots. (F) Comparison of the expression of the three identified genes among strains. mRNA abundance of each gene was compared with that of Wt cells, and the ratio was plotted.

analyze the null phenotype of these genes in $\Delta 8$ cells, we constructed natamycin (NatMX) gene cassettes that contained genes as well as 1-kb regions upstream and downstream of each gene (Fig. 3A). After transformation, colonies were selected from yeast extract-peptone-dextrose (YPD) plates containing 100 μ g/mL

NatMX and analyzed by colony PCR. We succeeded in recovering many colonies in which *SRX1* was deleted in both $\Delta 8$ and Wt cells (Fig. S1A); however, no $\Delta 8$ colonies were recovered with deletions of either *CCP1* or *UTH1*.

Coexpression of *CCP1* and *UTH1* Releases the Dependence on Aneuploidy. We designed a laboratory evolution experiment (31) to determine whether the disomy of chr-XI was selected for the increased expression of *CCP1* and *UTH1* in $\Delta 8$ cells. To this end, we prepared a $\Delta 8$ marker strain in which one of the two copies of *SRX1* was replaced with the NatMX marker (Fig. 3A). The evolution experiment was conducted by transforming the marker strain with plasmids carrying *SRX1*, *CCP1*, and *UTH1* under constitutive promoters either individually or in combination (Fig. S1B). Three independent colonies were selected from each transformation and grown on SDP medium with antibiotics for 120 generations (Fig. S1B), and populations were examined with a 25-generation increment. Strikingly, we observed spontaneous loss of chr-XI in all three lines of cells expressing *CCP1* + *UTH1* as well as lines expressing *CCP1* + *UTH1* + *SRX1* (Fig. 3), whereas neither expression of individual genes nor the combinations of *CCP1* + *SRX1* or *UTH1* + *SRX1* led to this outcome. These data suggested that both *CCP1* and *UTH1* are required for yeast cells deficient in thiol peroxidases.

Elevated Expression of Ccp1 in $\Delta 8$ Cells. We next used comparative 2D gel electrophoresis, because it allows a direct measure of the synthesis rate of about a third of all yeast soluble proteins (Ccp1 but not Uth1 was not detected by this approach) (Fig. 4A and Fig. S2). We found that in untreated $\Delta 8$ cells, the synthesis rate of Ccp1 was abnormally high (23.5-fold increase compared with Wt cells). The synthesis rate of Sod2 (8.6-fold), Trx2 (6.0-fold), and Sod1 (4.4-fold) was also increased, but not as much as that of Ccp1. Because these proteins are all part of the yeast H₂O₂-inducible response (32), their constitutive expression in $\Delta 8$ cells indicates a deregulated expression, possibly as a result of chronic oxidative stress. In comparison, Wt cell exposure to H₂O₂ led to an 8-fold synthesis rate increase of Ccp1, which did not match its very high expression levels seen in untreated $\Delta 8$ cells (Fig. 4B).

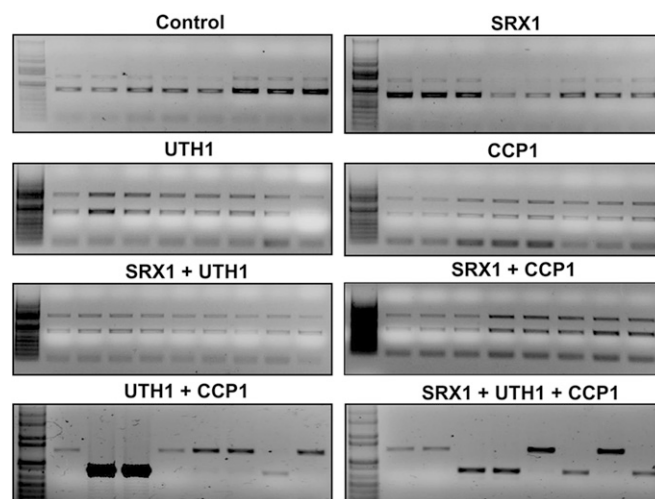


Fig. 3. Aneploidy is linked to elevated expression of *CCP1* and *UTH1*. Representative colonies from each expression group of the laboratory evolution experiment (Fig. S1) were analyzed at 120 generations by colony PCR. Increased expression of genes *CCP1* + *UTH1* or *CCP1* + *UTH1* + *SRX1* allows cells to lose the extra copy of chr-XI (two lower panels). Individual colonies expressing these genes lost one or the other copy of this chromosome, shown by the loss of the upper or lower bands. All colonies expressing individual genes or pairs of genes including *SRX1* had both bands. Left lanes in each panel show size markers.

proteomics data, H₂O₂ treatment led to a 6-fold increase in transcription and 12-fold increase in translation of Ccp1, but there was no change in Uth1 levels (Fig. 4B). Even though aneuploidy can introduce adaptive traits under certain conditions, organismal fitness occurs at the expense of slow proliferation. We tested this observation in our model and showed that losing the extra chromosome leads to a positive effect on $\Delta 8$ cells: The evolved $\Delta 8$ populations grew faster compared with the original mutant cells.

Overall, we have identified an example of adaptive dosage compensation where whole-chromosome duplication promotes increased expression of two genes and supports the growth of thiol peroxidase null strains. Our results clearly show that aneuploidy can rapidly compensate for the absence of major protectors against oxidative stress. It would be of interest to examine how this finding applies to multicellular organisms, considering that aneuploidy is highly detrimental for them. Oxidative stress and aneuploidy contribute to many pathological conditions, including different types of cancers. In this regard, experimental approaches addressing this relationship may bring fundamental insights into these processes and improve our ability to manipulate these systems for research and therapeutic purposes.

Materials and Methods

Yeast Strains and Plasmids. Isolation of mutant strains lacking all eight thiol peroxidases was reported previously (15, 17). Details regarding all strains used in the current study can be found in Table S1. Yeast strains were grown on YPD medium. The strain used in the laboratory evolution experiment was created by replacing one copy of *SRX1* (i.e., on one of the two chr-XIs) with a NatMX resistance (100 μ g/mL) cassette in a $\Delta 8$ strain. For expression of genes of interest, two plasmids were used. *SRX1* was cloned into the *pCEV* plasmid (39) containing Zeocin (ZeoMX) resistance, whose expression was controlled by the constitutive *TEF1* promoter. For expression of *CCP1* and/or *UTH1*, we modified a recently constructed triple-expression plasmid, *pATP425* (40), by inserting a bialaphos (PatMX) cassette along with a *TEF1* promoter and terminator at the *SacI*-*PacI* restriction sites. We inserted *CCP1* and/or *UTH1* sequences at the *SacI*-*NotI* and *PmeI*-*FseI* restriction sites, wherein their expression was controlled under the *TDH3* and *ADH1* promoters, respectively. PatMX (300 μ g/mL) and ZeoMX (100 μ g/mL) selection was performed on SDP medium (1 g/L proline, 6.7 g/L yeast nitrogen base, 20 g/L glucose). Cells were transformed with plasmids to express individual genes. After colonies were selected on both plates, combinatory transformations were performed and the colonies were selected on SDP media containing ZeoMX and PatMX for coexpression.

H₂O₂ Sensitivity and Analyses of Cell Growth. Cells were grown at 30 °C, and OD₆₀₀ measurements were taken at 15-min intervals using a Bioscreen C MBR instrument until cells reached early stationary phase. Resistance of Wt and mutant strains to H₂O₂ was determined with spot assays. For each strain, overnight cultures were adjusted to OD₆₀₀ 0.6, and 5 μ L of serial dilutions (10-fold each) was spotted on solid medium that contained H₂O₂ at the indicated concentrations. Cells were grown for 3 d at 30 °C and pictures were taken.

Dependence on Respiration. Sensitivity of yeast cells to antimycin-A, rotenone, and oligomycin was assessed with spot assays. Cultures were collected at OD₆₀₀ 0.6, and 5 μ L of 10-fold serial dilutions was spotted on solid medium containing 10 μ g/mL antimycin A, 20 μ g/mL rotenone, or 7.5 μ g/mL oligomycin. For

visualization of mitochondria under the microscope, logarithmically grown cells were washed three times with 1 \times saline buffer and incubated with calcofluor-white (Sigma) and MitoTracker Red (Invitrogen) in the same buffer for 30 min. Cells were washed and visualized under a fluorescence microscope. To assess a relative abundance of mtDNA in yeast strains, we calculated the read coverage of mitochondrial and nuclear genomes, and the abundance of mtDNA (X_{mt}) was plotted as the ratio of the coverage of X_{mt} and the nuclear genome (X_{nuc}) coverage for each strain.

Genome Sequencing and RNA-Seq Analysis. Genome sequencing and RNA-seq analyses were performed on various yeast strains as described previously (15, 38). We further used the Genome Analysis Toolkit to calculate the depth of coverage for each chromosome (41). The “DepthOfCoverage” tool was applied to sorted *.bam files to generate a genome-wide table of sequencing depth. A custom Perl script modified this table by omitting highly abundant mitochondrial sequences (>100 \times coverage than the nuclear genome) and ribosomal DNA (>50 \times than the rest of the nuclear genome). We also normalized the coverage by the total number of reads per sample. The graph was plotted with the ggplot2 package within the R statistical environment (42). Each dot is an average of the sequencing depths of 100 nt. There are 100,000 dots per graph. RNA-seq (FASTQ) files were aligned to the yeast reference genome; Ensembl build R64-1-1 was downloaded from the Illumina iGenome resource at support.illumina.com/sequencing/sequencing_software/igenome.html using Bowtie 2 v2.1.0 (43) and the spliced-read mapper TopHat (v2.0.9) (44), with reference gene annotations to guide the alignment (-G argument in TopHat). Fragments per kilobase of transcript per million mapped (FPKM) reads were calculated using Cufflinks v2.1.1 (45), with default parameters.

Laboratory Evolution Experiment. The laboratory evolution experiment was carried out by serial dilution. Cells were grown until reaching stationary phase at 30 °C with moderate shaking and then diluted by a factor of 1:500 with fresh SDP medium (~4.5 generations per dilution) containing ZeoMX and/or PatMX antibiotics. This procedure was repeated until loss of the extra chromosome was detected by colony PCR. Briefly, 10 μ L each culture was spread onto SDP plates containing ZeoMX and/or PatMX. After 2 d, several colonies were selected and incubated at 30 °C in 2.5 μ L water containing 20 U/mL zymolase-20T solution for 30 min and for 5 min at 95 °C in PCR tubes. A drop of mineral oil was added on top to prevent evaporation. After cooling on ice, 50 μ L water was added to each tube and 1.25 μ L was used as a template for PCR.

Analysis of Protein Expression. Strains were grown at 30 °C in YNB defined medium containing (wt/vol) 0.17% yeast nitrogen base, 0.5% ammonium sulfate, 2% glucose, supplemented with appropriate amino acids and 0.2 mM GSH. When OD₆₀₀ reached 0.35, H₂O₂ (0.6 mM) was added or not (t_0); at t_{20} (20 min), cells were pulse-labeled with [³⁵S]methionine (150 μ Ci), and at t_{40} (40 min) they were collected. Preparation of whole-cell protein extracts and 2D gel electrophoresis were performed as described (46). Dried gels were analyzed on a Storm 860 Molecular Imager, and spot intensity quantification was performed with ImageQuant software (GE Healthcare), as described (47). For select proteins, a synthesis rate index was calculated as the value of spot intensity signal normalized to total gel intensity signal.

ACKNOWLEDGMENTS. We thank Dr. Angelika Amon for a chr-XI aneuploid strain (Wt-M11), Dr. Gilles Lagniel for the proteome analysis, and Dr. Jun Ishii for providing the *pATP425* vector. This work was supported by NIH Grant GM065603 (to V.N.G.) and Grant PLBIO INCA_5869 from Agence Nationale pour la Recherche (ANR) ERRed and from Institut National du Cancer (InCa) (to M.B.T.).

- Apel K, Hirt H (2004) Reactive oxygen species: Metabolism, oxidative stress, and signal transduction. *Annu Rev Plant Biol* 55:373–399.
- Geiszt M, Kopp JB, Várnai P, Leto TL (2000) Identification of renox, an NAD(P)H oxidase in kidney. *Proc Natl Acad Sci USA* 97(14):8010–8014.
- Cross CE, et al. (1987) Oxygen radicals and human disease. *Ann Intern Med* 107(4):526–545.
- Rhee SG, Chae HZ, Kim K (2005) Peroxiredoxins: A historical overview and speculative preview of novel mechanisms and emerging concepts in cell signaling. *Free Radic Biol Med* 38(12):1543–1552.
- Finkel T (2011) Signal transduction by reactive oxygen species. *J Cell Biol* 194(1):7–15.
- Finkel T, Holbrook NJ (2000) Oxidants, oxidative stress and the biology of ageing. *Nature* 408(6809):239–247.
- Wood ZA, Schröder E, Robin Harris J, Poole LB (2003) Structure, mechanism and regulation of peroxiredoxins. *Trends Biochem Sci* 28(1):32–40.
- Park SG, Cha MK, Jeong W, Kim IH (2000) Distinct physiological functions of thiol peroxidase isoenzymes in *Saccharomyces cerevisiae*. *J Biol Chem* 275(8):5723–5732.
- Huang ME, Kolodner RD (2005) A biological network in *Saccharomyces cerevisiae* prevents the deleterious effects of endogenous oxidative DNA damage. *Mol Cell* 17(5):709–720.
- D’Errico M, Parlanti E, Dogliotti E (2008) Mechanism of oxidative DNA damage repair and relevance to human pathology. *Mutat Res* 659(1–2):4–14.
- Maynard S, Schurman SH, Harboe C, de Souza-Pinto NC, Bohr VA (2009) Base excision repair of oxidative DNA damage and association with cancer and aging. *Carcinogenesis* 30(1):2–10.
- Neumann CA, et al. (2003) Essential role for the peroxiredoxin Prdx1 in erythrocyte antioxidant defence and tumour suppression. *Nature* 424(6948):561–565.
- van Loon B, Markkanen E, Hübscher U (2010) Oxygen as a friend and enemy: How to combat the mutational potential of 8-oxo-guanine. *DNA Repair (Amst)* 9(6):604–616.
- Iraqi I, et al. (2009) Peroxiredoxin Tsa1 is the key peroxidase suppressing genome instability and protecting against cell death in *Saccharomyces cerevisiae*. *PLoS Genet* 5(6):e1000524.
- Kaya A, et al. (2014) Thiol peroxidase deficiency leads to increased mutational load and decreased fitness in *Saccharomyces cerevisiae*. *Genetics* 198(3):905–917.

16. Gorla GR, Malhi H, Gupta S (2001) Polyploidy associated with oxidative injury attenuates proliferative potential of cells. *J Cell Sci* 114(Pt 16):2943–2951.
17. Fomenko DE, et al. (2011) Thiol peroxidases mediate specific genome-wide regulation of gene expression in response to hydrogen peroxide. *Proc Natl Acad Sci USA* 108(7):2729–2734.
18. Nemoto S, Takeda K, Yu ZX, Ferrans VJ, Finkel T (2000) Role for mitochondrial oxidants as regulators of cellular metabolism. *Mol Cell Biol* 20(19):7311–7318.
19. Hughes TR, et al. (2000) Widespread aneuploidy revealed by DNA microarray expression profiling. *Nat Genet* 25(3):333–337.
20. Torres EM, et al. (2007) Effects of aneuploidy on cellular physiology and cell division in haploid yeast. *Science* 317(5840):916–924.
21. Rancati G, et al. (2008) Aneuploidy underlies rapid adaptive evolution of yeast cells deprived of a conserved cytokinesis motor. *Cell* 135(5):879–893.
22. Sheltzer JM, Amon A (2011) The aneuploidy paradox: Costs and benefits of an incorrect karyotype. *Trends Genet* 27(11):446–453.
23. Chen G, Rubinstein B, Li R (2012) Whole chromosome aneuploidy: Big mutations drive adaptation by phenotypic leap. *BioEssays* 34(10):893–900.
24. Biteau B, Labarre J, Toledano MB (2003) ATP-dependent reduction of cysteine-sulphinic acid by *S. cerevisiae* sulphiredoxin. *Nature* 425(6961):980–984.
25. Sels AA, Cocriamont C (1968) Induced conversion of a protein precursor into cytochrome C peroxidase during adaptation of yeast to oxygen. *Biochem Biophys Res Commun* 32(2):192–198.
26. Kwon M, Chong S, Han S, Kim K (2003) Oxidative stresses elevate the expression of cytochrome c peroxidase in *Saccharomyces cerevisiae*. *Biochim Biophys Acta* 1623(1):1–5.
27. Martins D, Kathiresan M, English AM (2013) Cytochrome c peroxidase is a mitochondrial heme-based H₂O₂ sensor that modulates antioxidant defense. *Free Radic Biol Med* 65:541–551.
28. Kissová I, Deffieu M, Manon S, Camougrand N (2004) Uth1p is involved in the autophagic degradation of mitochondria. *J Biol Chem* 279(37):39068–39074.
29. Kennedy BK, Austriaco NR, Jr, Zhang J, Guarente L (1995) Mutation in the silencing gene SIR4 can delay aging in *S. cerevisiae*. *Cell* 80(3):485–496.
30. Bandara PD, Flattery-O'Brien JA, Grant CM, Dawes IW (1998) Involvement of the *Saccharomyces cerevisiae* UTH1 gene in the oxidative-stress response. *Curr Genet* 34(4):259–268.
31. Elena SF, Lenski RE (2003) Evolution experiments with microorganisms: The dynamics and genetic bases of adaptation. *Nat Rev Genet* 4(6):457–469.
32. Godon C, et al. (1998) The H₂O₂ stimulon in *Saccharomyces cerevisiae*. *J Biol Chem* 273(35):22480–22489.
33. Lengauer C, Kinzler KW, Vogelstein B (1998) Genetic instabilities in human cancers. *Nature* 396(6712):643–649.
34. Hassold TJ, Jacobs PA (1984) Trisomy in man. *Annu Rev Genet* 18:69–97.
35. Selmecki A, Forche A, Berman J (2006) Aneuploidy and isochromosome formation in drug-resistant *Candida albicans*. *Science* 313(5785):367–370.
36. Daum G, Böhn PC, Schatz G (1982) Import of proteins into mitochondria. Cytochrome b2 and cytochrome c peroxidase are located in the intermembrane space of yeast mitochondria. *J Biol Chem* 257(21):13028–13033.
37. Camougrand NM, Mouassite M, Velours GM, Guérin MG (2000) The “SUN” family: UTH1, an ageing gene, is also involved in the regulation of mitochondria biogenesis in *Saccharomyces cerevisiae*. *Arch Biochem Biophys* 375(1):154–160.
38. Gerashchenko MV, Lobanov AV, Gladyshev VN (2012) Genome-wide ribosome profiling reveals complex translational regulation in response to oxidative stress. *Proc Natl Acad Sci USA* 109(43):17394–17399.
39. Vickers CE, Bydder SF, Zhou Y, Nielsen LK (2013) Dual gene expression cassette vectors with antibiotic selection markers for engineering in *Saccharomyces cerevisiae*. *Microb Cell Fact* 12:96.
40. Ishii J, et al. (2014) Three gene expression vector sets for concurrently expressing multiple genes in *Saccharomyces cerevisiae*. *FEMS Yeast Res* 14(3):399–411.
41. McKenna A, et al. (2010) The Genome Analysis Toolkit: A MapReduce framework for analyzing next-generation DNA sequencing data. *Genome Res* 20(9):1297–1303.
42. R Core Development Team (2015) R: A Language and Environment for Statistical Computing (R Foundation for Statistical Computing, Vienna). Available at <https://www.r-project.org>. Accessed March 1, 2015.
43. Langmead B, Salzberg SL (2012) Fast gapped-read alignment with Bowtie 2. *Nat Methods* 9(4):357–359.
44. Kim D, et al. (2013) TopHat2: Accurate alignment of transcriptomes in the presence of insertions, deletions and gene fusions. *Genome Biol* 14(4):R36.
45. Trapnell C, et al. (2012) Differential gene and transcript expression analysis of RNA-seq experiments with TopHat and Cufflinks. *Nat Protoc* 7(3):562–578.
46. Lee J, et al. (1999) Yap1 and Skn7 control two specialized oxidative stress response regulons in yeast. *J Biol Chem* 274(23):16040–16046.
47. Hasan R, et al. (2002) The control of the yeast H₂O₂ response by the Msn2/4 transcription factors. *Mol Microbiol* 45(1):233–241.